

Primary Response Assessment Method for Concept Design of Monotonous Thin-Walled Structures

V. Zanic, P. Prebeg

A concept design methodology for monotonous, tapered thin-walled structures (wing/fuselage/ship/bridge) is presented including modules for: model generation; loads; primary (longitudinal) and secondary (transverse) strength calculations; structural feasibility (buckling/fatigue/ultimate strength criteria); design optimization modules based on ES/GA/FFE; graphics. A method for primary strength calculation is presented in detail. It provides the dominant response field for design feasibility assessment. Bending and torsion of the structure are modelled with the accuracy required for concept design. A '2.5D-FEM' model is developed by coupling a 1D-FEM model along the 'monotony' axis and a 2D-FEM model(s) transverse to it. The shear flow and stiffness characteristics of the cross-section for bending and pure/restrained torsion are given, based upon the warping field of the cross-section. Examples: aircraft wing and ship hull.

Keywords: thin-walled structures, shear flow, FEM, concept design.

1 Introduction

The concept design methodology for monotonous, tapered, thin-walled structures (wing/fuselage/ship/bridge) is presented. The problem solution is based on the OCTOPUS program [1, 2]. It contains: (A) response and feasibility analysis modules (FIN-CREST), (B) decision making-synthesis modules (DeMak) and (C) interaction/visualization programs (MAESTRO MM/MG and DeVIEW) that iterate in the design cycle. The modules are summarized in Table 1 as modules 1a–8c.

(A) *The analytical (CREST) modules* and methods are fully described in [2]. Module-1a INDAT is used for data generation, combined with the MAESTRO FEM MODELER [8]. Module-2 LOAD is used for design load generation. Module-1b MIND is used for determining the minimal scantlings based on prescribed rules (LR, DnV, ABS, etc.) Module-3a LTOR is used for direct calculation of the primary strength (shear flow and corrected stresses in bending and warping torsion). They are calculated using an original extended beam theory [5, 6]. Module-3b TOKV is used for the transverse strength calculation (newly developed 8-node stiffened panel macro-elements are used for modeling the transverse structural response). Module-4 is the PANEL library of structural serviceability and ultimate strength criteria for the structural adequacy calculation [4], using the response fields generated in modules 3a and 3b. Module-8a is VB-SHELL for the designer-model interaction. Module-8b MAESTRO GRAPHIC [8] is used for presenting the model (loading, response, adequacy, etc.)

(B) *Synthesis (DeMak) modules* and methods are documented in [1, 3]. Local variables for substructures ($s = 1, \dots, NS$), are denoted $\underline{x}^s = \{x_i\}^s = \{t_{\text{plating}}, n_{\text{stiffeners}}, h_{\text{web}} \dots\}^s$. Substructure areas $\mathbf{X} = \{X_s\}$ are intermediate (global) variables, where $X_s = X_s(\underline{x}^s)$. Project k is defined as $\mathbf{P}^k = \{\underline{x}^1, \dots, \underline{x}^{NS}, \mathbf{x}_{\text{fixed}}\}^k$. Design criteria (attributes, objectives, constraints) are formulated as a library of mathematical func-

tions/procedures for driving the optimization process or feasibility check. OCTOPUS metamodeling of failure surfaces is based on the most unsatisfied constraint from each local problem. They are added to the set of global constraints. The value function for a global level is a multicriterion combination of normalized attribute functions. The solution strategy involves generation of designs, using (a) a Random Number Generator in the first cycles of design space exploration, and (b) Fractional Factorial Experiments for subsequent cycles. Coordination is performed by modifying $v(\underline{x}^s)$ respective to its divergence from globally optimal substructure area X^s . Special provisions:

- generation of promising designs using 27 designs obtained from Orthogonal Array L27.
- extensive usage of tables of optimized profiles to speed up the generation process.

Modules 6 and 7c (GAZ) are used for calculating the sensitivity of the structural response with respect to the design variables, based on the global strength module FIN/LTOR [7]. Module-7a GLO is used for global level MODM optimization (level 1) of the cross-section. Module-7b LOC is used for local coordinated MADM decision making via sequential application of stochastic search methods and Theory of experiments.

(C) *Module-8c DeVIEW* is used for the designer-model interaction with graphic presentation of designs in the design and attribute spaces. The stratified distances from the target (or the ideal) design, calculated by L_p metric are used as a means of visualizing the multidimensional space of the design attributes and/or free variables. Visualization is the most powerful tool for the designer's understanding of the Decision Support Problem. It generates expert knowledge about the problem for all participants involved, and helps the designer to identify advantageous combinations of variables, feasible options and clusters of non-dominated designs (Pareto frontier, thus enabling realistic decision support to the head and structural designer).

Table 1: Summary of OCTOPUS modules

MODULE	OCTOPUS
(1a) STRUCTURAL MODEL	MAESTRO files generated by program MM and used in OCTOPUS (s/r INDAT)
(2) LOAD MODEL	Rule Loads + designer given loads generated automatically by OCTOPUS s/ r LOAD
(1b) MINIMAL DIMENSIONS	Minimal dimensions by OCTOPUS s/r MIND
(3a) RESPONSE CALCULATIONS - - PRIMARY STRENGTH (u- displ.; stresses σ_x, τ)	Extended beam theory (cross section warping fields in bending and torsion, normal stresses s, respective shear flows) program LTOR
(3b) RESPONSE CALCULATION - - TRANSVERSE STRENGTH (displacements v, w, θ x stresses σ_y)	FEM calculation using beam element with or without rigid ends and stiffened panel macroelements program TOKV
(4) FEASIBILITY CALCULATION $g_i = \frac{C_i - D_i}{C_i + D_i}$ (Normalized Safety Factor)	Calculation of macroelement feasibility using library of safety criteria in program PANEL (C – capability; D – Demand from 3a and 3b)
(5) RELIABILITY CALCULATION (not used)	FORM approach to panel reliability. Upper Dietlevsen bound as design attribute
(6) DECISION SUPPORT PROBLEM DEFINITION (interactive)	Constraints: User given Minimal dimensions Library of criteria (see 4) Objectives: minimal weight, minimal cost, maximal safety
(7a, b, c) OPTIMIZATION METHOD	Decision making procedure using a) Global MODM optimization program GLO b) Local MADM optimization module LOC c) Coordination module GAZ
(8a, b, c) PRESENTATION OF RESULTS	a) VB Environment, b) Program MG, c) DeVIEW graphic tool

2 Modeling philosophy for primary response in concept design

Classical FE modeling, giving good insight into stresses and deformations, is not capable of giving the efficient and fast answers regarding feasibility criteria (buckling, fatigue, yield) required by the Rules. However, structural feasibility and compliance with the Rule requirements are of primary interest, not stresses or deformations.

Most of the local failure criteria, e.g. various buckling failure modes of stiffened panels, require specified force and displacement boundary conditions. They are available only if logical structural parts, such as complete stiffened panels between girders and frames, are modeled (macro-elements).

For the concept design structural evaluation of the primary response (longitudinal strength, torsional strength), the beam idealization of a wing/ship/bridge is often used. A primary strength calculation provides the dominant response field (Demand) for design feasibility assessment. The evaluation is based on extended beam theory, which needs cross-sectional characteristics. These are obtained using analytical methods, which can be very complicated for real combinations of open and closed cross-sections.

Application of energy based numerical methods gives an opportunity for an alternative approach to the given problems. The method is based on decomposing a cross-section into the line finite elements between nodes i and j with coordinates $(y_i, z_i), (y_j, z_j)$; element thickness t^e ; material characteristics (Young's modulus E /shear modulus G); material

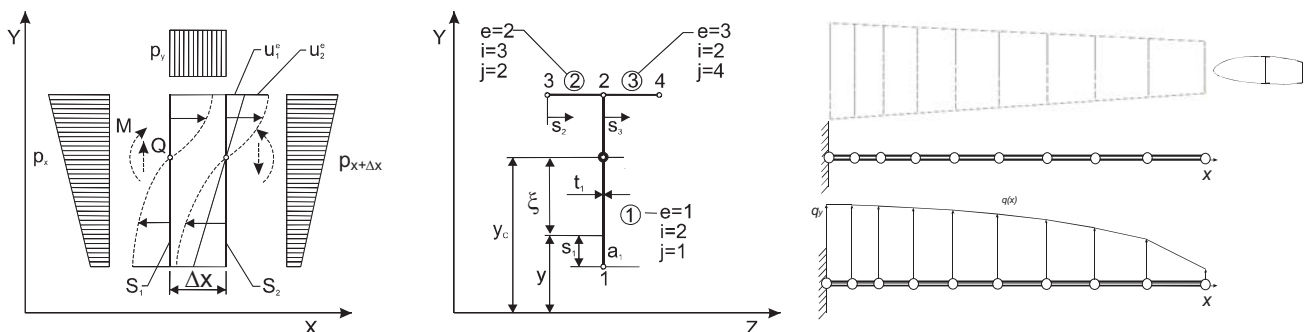


Fig. 1: Transverse strip (S1-S2) with external loading p, warping fields u and 1D/2D FEM idealization

ters the element axial, bending and torsion parameter distributions, based on the applied shape functions, can be derived (e.g. $\theta(x)$, $\theta_{,x}(x)$, $\theta_{,xx}(x)$, $\theta_{,xxx}(x)$ for torsion). The key element for calculation of the response of the complex thinwalled structure is therefore determination of elements of \mathbf{G}^x . A simple and elegant FEM procedure for such a calculation is presented in the sequel.

3 Calculation of response for a transverse strip with a complex cross section

The shear flow and geometrical characteristics of the cross section in bending and torsion is usually calculated using analytical methods. Such calculations become rather complicated for multiple-connected cross section graphs with a combination of open and closed (cell) contours. Application of numerical methods based on the energy approach offers an elegant alternative. The procedure is based on section decomposition into finite elements, as first introduced by Herman and Kawai. In the sequel, the method of calculation as described in [5, 6] is presented. It has been successfully used in practical calculations since its development for [10]. The simplest decomposition of thin-walled cross-section (symmetric or not) into line finite elements (segments) is shown in Figs. 1 and 2. These elements form stiffened panel macro-elements for the feasibility evaluation.

The methodology is based on applying the principle of minimum total potential energy (Π) with respect to parameters which define the displacement fields of the structure. The primary displacement field (following classical beam theory) is defined via displacements and rotations of the cross section as a whole. Secondary displacement field $\mathbf{u}_2(x, y, z) \equiv \mathbf{u}(x, y, z)$ represents warping (deplanation) of the cross section. For piecewise-linear FEM idealization of the cross-section, divided into n elements, with shape functions \mathbf{N} in the element coordinate system (x, s) , the warping field reads:

$$u(s)_{x=x_0}^e = \mathbf{N}^T \cdot \mathbf{u}^e = \left\{ 1 - \frac{s}{l^e} \quad \frac{s}{l^e} \right\} \begin{Bmatrix} u_i \\ u_j \end{Bmatrix}.$$

Element strain and stress fields ϵ and σ are obtained from the strain-displacement and stress-strain relations:

$$\epsilon \rightarrow \gamma_{xs} = \frac{\partial u}{\partial s} = \mathbf{B}^T \cdot \mathbf{u}^e = \left\{ -\frac{1}{l^e} \quad \frac{1}{l^e} \right\} \begin{Bmatrix} u_i \\ u_j \end{Bmatrix}, \text{ and}$$

$$\sigma \rightarrow \tau_{xs} = G^e \gamma_{xs} = G^e \mathbf{B}^T \cdot \mathbf{u}^e.$$

The total potential energy of the Δx -long transverse strip of the beam, with the cross-section divided into n elements, reads:

$$\begin{aligned} \Pi &= \sum_n \left[\int_{V^e} \sigma^T \epsilon \, dV - \int_{S^e} p(x,s) u(s) \, dS \right] \\ &= \sum_e \left[\int_{V^e} \frac{1}{2} \mathbf{B}^T \mathbf{B} \, dV - \int_{S^e} F(s) u(s) \, dS \right] \\ &= \Delta x \sum_e \left[\frac{1}{2} \mathbf{u}^{eT} \mathbf{K}^e \mathbf{u}^e - \mathbf{u}^{eT} \mathbf{F}^e \right], \end{aligned}$$

where $p(x,s)$ is the external loading on two cross sections (S_1 and S_2) of the strip. Minimization of Π leads to the classical FEM matrix relation $\mathbf{K}_{2D} \mathbf{u}_{2D} = \mathbf{F}_{2D}$ (shortened to $\mathbf{K} \mathbf{u} = \mathbf{F}$). The element stiffness matrix for the proposed linear displacement distribution along the line element (the same for bending and torsion) reads:

$$\mathbf{K}^e = \frac{G^e \cdot t^e \cdot RS^e}{l^e} \begin{bmatrix} 1 & -1 \\ -1 & 1 \end{bmatrix},$$

where RS is the prescribed shear efficiency.

4 Cross-sectional shear stress distribution due to bending

In the case of bending, the net external load (due to bending moments $M(x+\Delta x)$ and $M(x)$) is the normal stresses:

$$\begin{aligned} p(x,s) &= \sigma(x+\Delta x, s)_{S_2} - \sigma(x, s)_{S_1} = \frac{\partial}{\partial x} \sigma(x, s) \Delta x \\ &= Q(x) \frac{\xi_C(s)}{I(x)} \Delta x, \end{aligned}$$

where $\xi_C(s)$ is distance from the point to N. A.

The load vector for a nonsymmetrical cross-section in, e.g., bending about the z axis reads:

$$\begin{aligned} \mathbf{F}_z^e(x) &= Q_y(x) \cdot \bar{\mathbf{F}}_z^e(x) = \frac{E^e \cdot Q_y(x) \cdot t^e \cdot RN^e}{E(I_Y I_Z - I_{YZ}^2)} \\ &\cdot \left[I_Y \cdot \begin{Bmatrix} \frac{y_{iC} \cdot l^e}{2} + \frac{l^{e2} \sin \alpha^e}{6} \\ \frac{y_{iC} \cdot l^e}{2} + \frac{l^{e2} \sin \alpha^e}{3} \end{Bmatrix} - I_{YZ} \cdot \begin{Bmatrix} \frac{z_{iC} \cdot l^e}{2} + \frac{l^{e2} \sin \alpha^e}{6} \\ \frac{z_{iC} \cdot l^e}{2} + \frac{l^{e2} \sin \alpha^e}{3} \end{Bmatrix} \right]. \end{aligned}$$

For bending around the Y and Z axes, the matrix relations $\mathbf{K} \mathbf{u} = \mathbf{F}$ with $\mathbf{u} = Q(x) \cdot \bar{\mathbf{u}}$ can be converted into expressions for the warping due to unit load $\bar{\mathbf{F}}$. For node warping $u_i(x)$, unit warping $\bar{\mathbf{u}}(x)$ must be multiplied by $Q(x)$. This enables the assessment of shear stresses τ_Y^e or τ_Z^e from the expression $\tau^e = G(u_{2j} - u_{2i})/l^e$ in each element e between nodes i and j .

If necessary, it is possible to calculate shear stress distribution $\tau_{xs}^e(s)$ more accurately, from the mean stress τ_{xs}^{ke} obtained from FEM, and the contribution to each element calculated analytically $(\tau_{xs}^e(s))_u = (\tau_{xs}^{ke})_u - \tau_{1u}^{ke} + \tau_{1u}(s)$ $u = y$ or z from expression (for symmetrical section):

$$\begin{aligned} (\tau_{xs}^e(s))_z &= Q_z \cdot \left[G^e \cdot \mathbf{B}^T \cdot \bar{\mathbf{u}}_y^e - \frac{E^e \cdot RN^e}{EI_Y} \right. \\ &\cdot \left. \left(\frac{l^e}{3} \left(z_{iC} + \frac{1}{2} z_{yC} \right) - z_{iC} \cdot s - (z_{jC} - z_{iC}) \cdot \frac{s^2}{2l^e} \right) \right]. \end{aligned}$$

In this case, the sectional characteristics and shear center are easily obtained. The shear/torsion center position reads:

$$Y_{SC} = \sum_n \left[\int_0^{l^e} \tau_Z^e t^e d_C^e \, ds \right]_{Q_Z=1}, \quad Z_{SC} = \sum_n \left[\int_0^{l^e} \tau_Y^e t^e d_C^e \, ds \right]_{Q_Y=1},$$

where d_C^e is the normal distance from the centroid to e .

The shear stiffness for bending about the Y and Z axes, G_{AV} , G_{AH} reads:

$$GA_V = \left[\sum_e \left[\int_0^{l^e} \frac{((\tau_{xs}^e)_y)^2}{G^e} \cdot t^e \cdot ds \right] \cdot RS^e \right]^{-1};$$

$$GA_H = \left[\sum_e \left[\int_0^{l^e} \frac{((\tau_{xs}^e)_z)^2}{G^e} \cdot t^e \cdot ds \right] \cdot RS^e \right]^{-1}.$$

5 Corrected normal stresses due to the influence of shear (shear lag)

The normal stress must be corrected for (a) stress arising from a longitudinal change of the warping field and (b) normal stress due to correcting bending moment (M^c), compensating for the loss of cross section equilibrium:

$$(a) (\sigma_x^c)_y^i = \mathbf{E} \boldsymbol{\varepsilon} = E^e \left(\frac{\partial u}{\partial x} \right)_y^i = -E^e \cdot p_z \cdot (\bar{u}_y^i - \bar{u}_y^c) \cdot RN^e;$$

$$(b) M_y^c = \sum_e \int_0^{l^e} (\sigma_x^c)_y \cdot z_c(s) \cdot t^e \cdot ds.$$

The total normal stress correction in node i reads:

$$(\sigma_x^{cT})_y^i = RN^e \left[\frac{I_Z \cdot z_{iC} - I_{YZ} \cdot y_{iC}}{E(I_Y I_Z - I_{YZ}^2)} M_y^c E^e - E^e p_z (\bar{u}_y^i - \bar{u}_y^c) \right].$$

The approximate value of normal stress for simultaneous bending about axes y and z for node I reads:

$$\sigma_x^i = \left[RN^e \frac{M_Z}{EI_Z} E^e \cdot y_{iC} + (\sigma_x^{cT})_z^i \right] + \left[RN^e \frac{M_Y}{EI_Y} E^e \cdot z_{iC} + (\sigma_x^{cT})_y^i \right].$$

6 Calculation of warping and primary shear stresses due to pure torsion

A transverse strip of a thin-walled beam of length Δx is subjected to torsional loading. The displacement field of the middle line of thin walled elements can be expressed using the warping function $\bar{u}(s)_{t=0}$, rotation $v_s(x)_{t=0}$ around the centre of twist, twist rate $(\theta_{x,x})$ and angle (θ_x) of the twist reads:

$$u(x, s) = \bar{u}(s)_{t=0} \cdot \theta_{x,x}(x_0),$$

$$v(x, s, t) \rightarrow v_s(x)_{t=0} = d_{Tt=0} \cdot \theta_x(x_0),$$

where d_T is the normal distance from the element to the center of torsion. The strain (with $\varepsilon_s \approx 0$) and stress fields read:

$$\boldsymbol{\varepsilon} = \begin{Bmatrix} \varepsilon_x \\ \gamma_{xs} \end{Bmatrix} = \begin{Bmatrix} \bar{u} \cdot \theta_{x,xx} \\ \left(\frac{\partial \bar{u}}{\partial s} + d_T \right) \theta_{x,x} \end{Bmatrix},$$

$$\boldsymbol{\sigma} = \mathbf{E} \boldsymbol{\varepsilon} = \begin{Bmatrix} E \cdot \bar{u} \cdot \theta_{x,xx} \\ G \cdot \left(\frac{\partial \bar{u}}{\partial s} + d_T \right) \theta_{x,x} \end{Bmatrix}.$$

The total potential energy of a section is given by the standard expression:

$$\Pi = U - W = \int_V \frac{1}{2} \boldsymbol{\sigma}^T \boldsymbol{\varepsilon} dV - W.$$

After summation of all elements and transformation of local element displacements $\bar{\mathbf{u}}^e = \mathbf{N}^T \cdot \bar{\mathbf{u}}$ and loads \mathbf{F}^e into global displacements $\bar{\mathbf{u}}$ and loads \mathbf{F} we get:

$$U = \Delta x \cdot \theta_{x,x}^2 \cdot \left(\frac{1}{2} \bar{\mathbf{u}}^T \mathbf{K} \bar{\mathbf{u}} - \bar{\mathbf{u}}^T \mathbf{F} + \frac{1}{2} \sum_e RS^e \cdot d_T^2 \cdot l^e \cdot t^e \cdot G^e \right).$$

$$\text{Where } \mathbf{K}^e = RS^e \cdot G^e \cdot t^e \int_0^{l^e} \mathbf{B} \mathbf{B}^T ds,$$

$$\text{and } \mathbf{F}^e = -RS^e \cdot G^e \cdot t^e \cdot d_T^2 \int_0^{l^e} \mathbf{B} ds.$$

Minimization of total potential energy leads to two sets of equations:

$$(1) \quad \delta \Pi_{\theta'} = 0 \text{ (1D beam torsion) and}$$

$$(2) \quad \delta \Pi_{\bar{\mathbf{u}}} = 0 \text{ (2D cross-section warping).}$$

A second set of equations, $\delta \Pi_u = \delta U_u = 0 \rightarrow \mathbf{K} \bar{\mathbf{u}} = \mathbf{F}$, enables determination of the unit warping field.

The primary shear stresses on the elements which are parts of closed contours (cc) and open sections (os) can now be calculated as functions of 1D twist rates $\theta_{x,x}(x)$ (to be obtained from the first relation for 1D beam torsion):

$$\tau_{xs}^{ke(cc)} = G^e \cdot \theta_{x,x} \left(\left\{ -\frac{1}{l^e} \quad \frac{1}{l^e} \right\} \begin{Bmatrix} \bar{u}_i \\ \bar{u}_j \end{Bmatrix} + d_T^e \right) \text{ and}$$

$$\tau_{xs}^{ke(os)} = G^e \cdot \theta_{x,x} \frac{t^e}{2}.$$

7 Calculation of torsional and warping stiffness of thin-walled structures

To solve the equation for 1D beam free torsion, the torsional stiffness of elements which are parts of the open e_o and closed cells e_c can now be calculated using the known unit warping field $\bar{\mathbf{u}}$:

$$GI_{T_o} = \sum_{e_o} G^e \frac{l^e t^e^3}{3} RS^e,$$

$$GI_{T_c} = \sum_{e_c} G^e \cdot l^e \cdot t^e \cdot \left(\frac{\bar{u}_j - \bar{u}_i}{l^e} + d_T^e \right)^2 \cdot RS^e \text{ and}$$

$$GI_T = GI_{T_o} + GI_{T_c}.$$

Warping stiffness is calculated using the expression:

$$EI_W = \sum_e E^e \frac{l^e t^e}{3} (\bar{u}_i^2 + \bar{u}_i \cdot \bar{u}_j + \bar{u}_j^2) \cdot RN^e.$$

Using GI_T and EI_W , the matrix \mathbf{K}_{1D} for the 1D beam problem can be formed and relevant parameter distributions $\theta(x)$, $\theta_{x,x}(x)$, $\theta_{x,xx}(x)$, $\theta_{x,xxx}(x)$ can be determined for use in shear stress calculations.

8 Normal and secondary shear stresses due to restrained warping

Restrained warping of a thin-walled beam will induce (a) normal stresses in a cross-section and (b) secondary shear stresses which will balance the longitudinally non-uniform distribution of normal stresses. This additional mechanism will influence the strain energy and the work of expression, so an iterative solution may be needed for greater accuracy.

Let $u(x, s) = \bar{u}(s) \cdot \theta_{x,x}(x)$ be the warping field in the cross-section calculated from the case of free torsion. Normal stresses are caused by restraining the warping, and vary along the x axis. They are given by:

$$\sigma_{xw} = E \cdot \epsilon_x = E \cdot \frac{\partial}{\partial x} (\bar{u}(s) \cdot \theta_{x,x}(x)) \text{ or}$$

$$\sigma_{xw}^i = E^e \cdot \theta_{x,xx} \cdot \bar{u}_i \cdot RN^e.$$

Let $u_2(x, s)$ be the secondary displacement field containing a displacement correction due to restrained warping. The total potential energy of a transverse strip consists of the internal energy generated from the fields ϵ_2 and σ_2 (based on u_2) and the additional work done by the strip axial load p_x on the secondary displacements u_2 . If the change of u_2 along strip length Δx is neglected, the total potential energy reads:

$$\Pi = \sum_e \Pi^e = \sum_e \left[\frac{1}{2} \int_{V^e} G^e \left(\frac{\partial u_2}{\partial s} \right)^2 dV - \Delta x \int_{S_2^e} \frac{\partial p_x}{\partial x} u_2(x, s) dS \right].$$

The net external load Δp_x due to restrained warping reads:

$$\Delta p_x(x, s) = -\Delta \sigma_{xw}(x, s) = -E^e \cdot \bar{u}(s) \cdot \theta_{x,xxx}(x) \cdot RN^e \cdot \Delta x,$$

and the total potential energy of the element, using the same shape functions as before, reads:

$$\Pi^e = \frac{1}{2} \Delta x \cdot \mathbf{u}_2^e \mathbf{T} \left(t^e \cdot G^e \cdot RS^e \int_0^{l^e} \mathbf{B} \mathbf{B}^T ds \right) \cdot \mathbf{u}_2^e$$

$$+ \Delta x \cdot \mathbf{u}_2^e \mathbf{T} \left(\theta_{x,xxx} \cdot t^e \cdot E^e \cdot RN^e \int_0^{l^e} \mathbf{N} \mathbf{N}^T ds \right) \cdot \bar{\mathbf{u}}^e.$$

Minimization of the total potential energy with respect to the unknown displacement field u_2 leads to:

$$\delta \Pi_{u_2} = 0 \rightarrow \Delta x (\mathbf{K} \mathbf{u}_2 + \mathbf{F}) = 0 \rightarrow \mathbf{K} \bar{\mathbf{u}}_2 = -\mathbf{F},$$

where: \mathbf{K} is the global stiffness matrix as before, \mathbf{u}_2 is the global vector of unknown displacements $\mathbf{u}_2 = \theta_{x,xxx} \cdot \bar{\mathbf{u}}_2$, \mathbf{F} is the global load vector $\mathbf{F} = \theta_{x,xxx} \cdot \bar{\mathbf{F}}$. The element load and the secondary shear stresses (constant on element) read:

$$\mathbf{F}^e = \theta_{x,xxx} \cdot RN^e \cdot E^e \cdot t^e \cdot l^e \begin{bmatrix} 1/3 & 1/6 \\ 1/6 & 1/3 \end{bmatrix} \begin{Bmatrix} \bar{u}_i \\ \bar{u}_j \end{Bmatrix} = \theta_{x,xxx} \bar{\mathbf{F}}^e ;$$

$$\tau_{xs}^{ke(2)} = G^e \frac{\partial u_2}{\partial s} = G^e \frac{u_{2j} - u_{2i}}{l^e} = G^e \frac{\bar{u}_{2j} - \bar{u}_{2i}}{l^e} \cdot \theta_{x,xxx}.$$

The shear stress distribution can be calculated more accurately along the element (similar to the bending case) from the known element average stress $\tau_{xs}^{ke(2)}$, the direction of shear stress flow, local element contribution $\tau_2(s)$ and its

average τ_2^{ke} using expression $\tau_{xs}^{e(2)}(s) = \tau_{xs}^{ke(2)} - \tau_2^{ke} + \tau_2(s)$. After rearranging, it reads:

$$\tau_{xs}^{e(2)}(s) = \left[G^e \frac{\bar{u}_{2j} - \bar{u}_{2i}}{l^e} + \frac{E^e \cdot RN^e}{RS^e} \left((\bar{u}_i + \frac{1}{2} \bar{u}_j) \frac{l^e}{3} - \bar{u}_i \cdot s - \frac{\bar{u}_j - \bar{u}_i}{2l^e} s^2 \right) \right] \cdot \theta_{x,xxx}.$$

9 Examples

The first example is based on reports from the Advanced Subsonic Technology (AST) program. In the course of this program an experimental model of a composite wing box was made and tested (Fig. 3). [11] gives the loads carried by the hydraulic actuators which simulate the in-flight loading conditions.

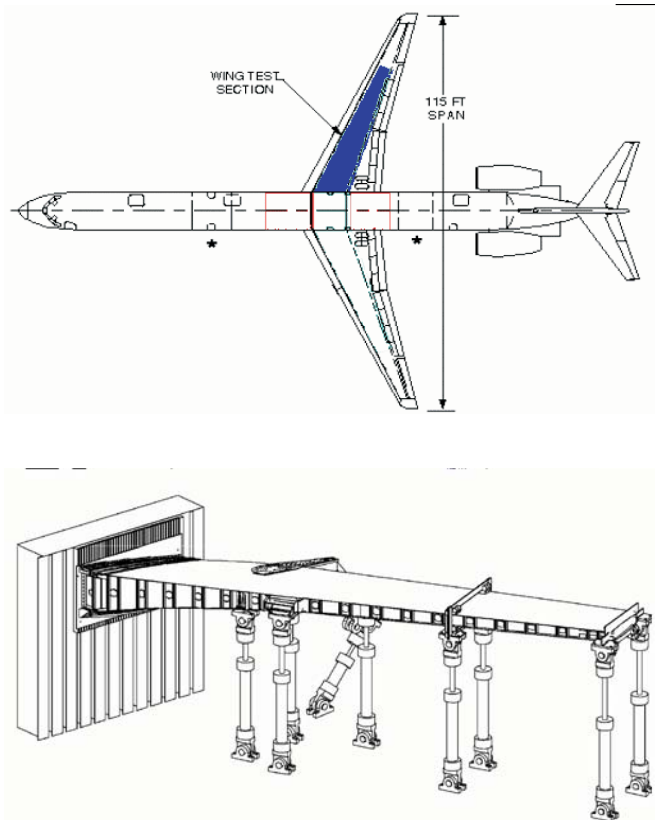


Fig. 3: MD 90 airplane and the test model of the wing box

The example shows a way of rapidly modeling and calculating the overall response of a similar metal wing box with linear behavior during the early stages of wing structural design. The analyzed wing box with reference to the AST box was shortened to 9.8 meters and modeled with high strength aluminum alloy 7075. The loads are decreased for the shortened wing box. The wing box is modeled by OCTOPUS 1D/2D combination.

Fig. 4 presents a model of the aluminum wing-box under modified +2.5G loading conditions, and the unit response which needs to be multiplied by the values in parentheses to get the actual values for the considered load. The response components are decoupled to show the influence of each type

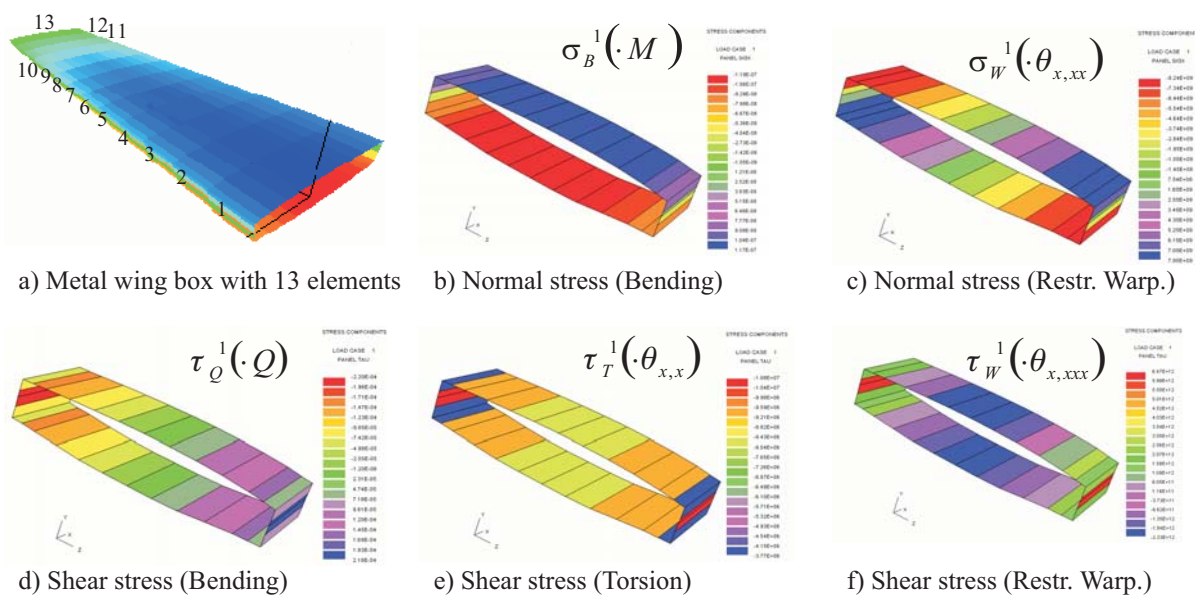
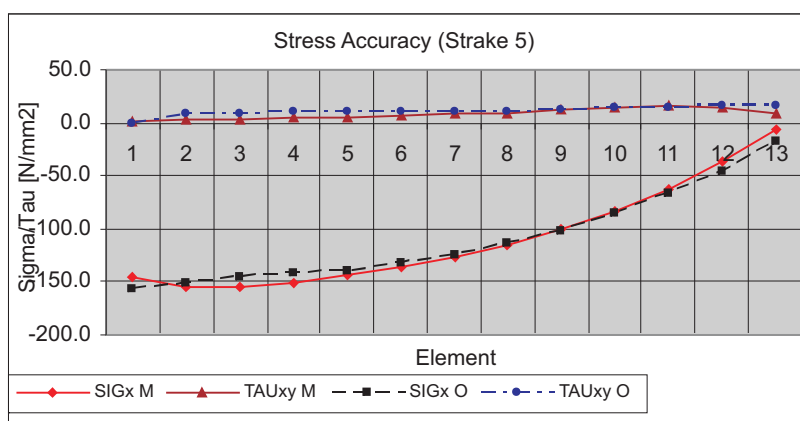


Fig. 4: Wing box model and unit responses of 1D FEM element 10 (between ribs 10 and 11)



(a)

1D-Element 10	
y_{CG} [mm]	-14.5818
z_{CG} [mm]	-337.763
φ [°]	7.14E-02
y_{SC} [mm]	-16.4946
z_{SC} [mm]	-354.305
A [mm ²]	66270
I_y [mm ⁴]	2.78E+10
I_z [mm ⁴]	1.66E+09
I_{yz} [mm ⁴]	3.26E+07
I_1 [mm ⁴]	2.78E+10
I_2 [mm ⁴]	1.66E+09
I_t [mm ⁴]	3.96E+09
I_w [mm ⁶]	2.85E+14
A_v [mm ²]	2412.777
A_h [mm ²]	31405.07

(b)

Fig. 5: (a) Stress accuracy across a wing span between Octopus (O) and Maestro (M), (b) cross-sectional properties of 1D-FEM element 10

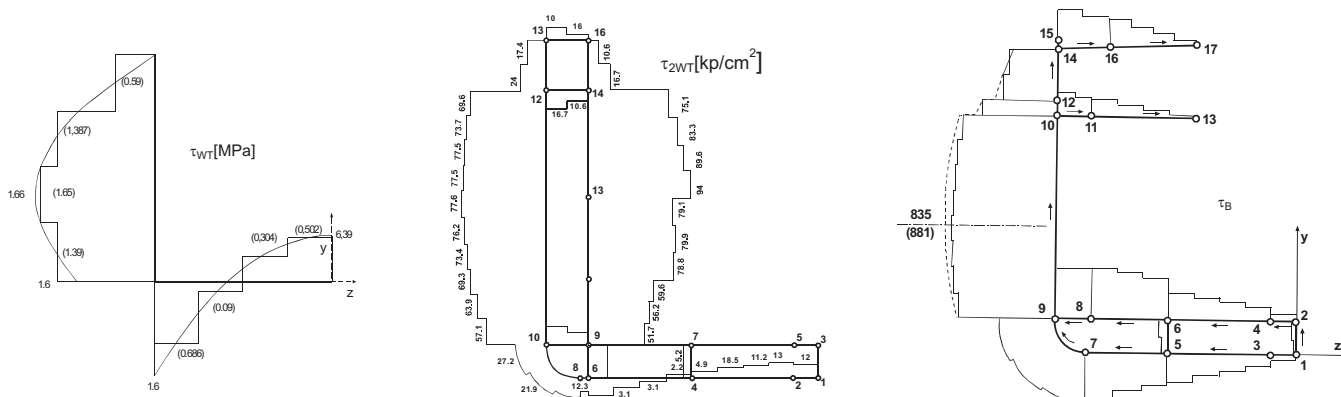


Fig. 6: (a) U-beam shear stress τ_W , (b) container ship shear stress τ_{Wr} , (c) general cargo ship shear stress τ_{Bvert}

of load on the response. The cross section geometric characteristics obtained from 2D FEM and used in 1D FEM analysis are given in Fig. 5b.

The accuracy of the method is demonstrated in Figures 5a and 6. Strake 5 of Fig. 5a is located in the middle of the upper skin. Fig. 6 presents the application to the U-channel and two standard ship structures. It can be seen that the accuracy of the shear stress distribution based on FEM (constant per element) and analytical formulae (continuous line) in examples 6a and 6c is very good, even without parabolic correction. The verification examples are taken from [5].

10 Conclusions

A simple and practical method for calculating the primary response of monotonous structures (wings, ships, bridges) has been presented. All cross-section parameters are easily determined for complex stiffened thin-walled structures using a special FEM procedure. It could successfully replace classical, often cumbersome, analytical calculations. The method has been in constant use since 1980, applied to many real structures for concept design (in the OCTOPUS system) or as the generator of the force boundary conditions for partial 3D FEM models.

References

- [1] Zanic, V., Das, P. K., Pu, Y., Faulkner, D.: "Multiple Criteria Synthesis Techniques Applied To Reliability Based design of SWATH Ship Structure." (Chapter 18). In: Integrity of Offshore Structures 5, (Faulkner, Das, Incecik, Cowling, editors), EMAS Scientific Publications, Glasgow, 1993, p. 387–415.
- [2] Zanic, V., Rogulj, A., Jancijev, T., Bralic, S., Hozmec, J.: "Methodology for Evaluation of Ship Structural Safety." Proc. of 10th Intl. Congress IMAM 2002, Crete, Greece, 2002, p. 54 + CD.
- [3] Zanic, V., Andric, J., Frank, D.: "Structural Optimization Method for the Concept Design of Ship Structures." Proceedings of the 8th International Marine Design Conference, Vol. 1; Papanikolau, A. D. (ed.), Athens, Greece, 2003., p. 99–110.
- [4] Hughes, O. F.: *Ship Structural Design*. Wiley, 1983, SNAME 1992.
- [5] Zanic, V.: "Calculation of Shear Flow in Cross-Section of Ship in Bending." (in Croatian). Proc. of Sorta Conference: Theory and practice in Shipbuilding, Split, Croatia, 1982.
- [6] Zanic, V.: "Determinazione Degli Sforzi Principali -Flessione e Torsione-Sollo Scafo di una nave Applicando Particolari Elementi Finiti." *Technica Italiana (Rivista D'Ingegneria)*, No.3, 1985, p. 105–113.
- [7] Prebeg, P.: Diploma thesis, University of Zagreb, 2003.
- [8] MAESTRO Documentation, Proteus Eng. Stevensville, MD, USA, 2003.
- [9] CREST Documentation, Croatian Register of Shipping, Split, Croatia, 2004.
- [10] Hughes, O. F., Mistree, F., Zanic, V.: "A Practical Method for the Rational Design of Ship Structures." *Journal of Ship Research*, Vol. 24 (1980), No. 2, June 1980, p. 101–113.
- [11] Karal, M.: *AST Composite Wing Program – Executive Summary*, NASA CR 2001-210650, 2001.

Vedran Zanic
phone: +385-1-6168122
fax: +385-1-6168399
e-mail: vedran.zanic@fsb.hr

Pero Prebeg
e-mail: pero.prebeg@fsb.hr

University of Zagreb
Faculty of Mechanical Engineering
and Naval Architecture
I. Lucica 5
10000 Zagreb, Croatia